REPORT DOCUMENTATION PAGE

AFOSR-TR-97 0106

1. AGENCY USE ONLY (Leave blank)	2. REPORT DATE	3. REPORT TYPE AND DATES COVERED
	02-03-97	Final Report 09-01-95 to 01-31-97

4. TITLE AND SUBTITLE
Transport and Relaxation of Lubricant Fluids at High Pressure

5. FUNDING NUMBERS
61103D 3484 XS

6. AUTHOR(S)
J. Jonas and L. Ballard

7. PERFORMING ORGANIZATION NAME(S) AND ADDRESS(ES)
Univ of Illinois - Urbana Champaign
801 South Wright Street
Champaign, IL 61820-6242

8. PERFORMING ORGANIZATION REPORT NUMBER

9. SPONSORING/MONITORING AGENCY NAME(S) AND ADDRESS(ES)
AFOSR/~~NC~~NL
Building 410, Bolling AFB DC
20332-6448
MAJ DeLong

10. SPONSORING/MONITORING AGENCY REPORT NUMBER
F49620-93-1-0555

11. SUPPLEMENTARY NOTES

12a. DISTRIBUTION/AVAILABILITY STATEMENT
APPROVED FOR PUBLIC RELEASE; DISTRIBUTION IS UNLIMITED.

12b. DISTRIBUTION CODE

13. ABSTRACT *(Maximum 200 words)*

The major focus of this project was on the construction and testing of high pressure, high resolution multinuclear NMR probe with unique performance features which permits measurements up to 10 kbar. Several experimental NMR studies of confined fluids of methylcyclohexane; perfluoromethylcyclohexane; ethanol; 2,2,2-trifluoroethanol; propionic acid and pentafluoropropionic acid were finished. These studies provided information on the effect of fluorination on the dynamic behavior of selected model liquids confined to porous silica glasses. In addition, natural abundance ^{31}C NMR relaxation study of the dynamics of polyfluorinated alkyl ether lubricant fluids was carried out.

14. SUBJECT TERMS
High pressure, NMR; Viscosity, Lubricants, Confined Fluids

15. NUMBER OF PAGES

16. PRICE CODE

17. SECURITY CLASSIFICATION OF REPORT	18. SECURITY CLASSIFICATION OF THIS PAGE	19. SECURITY CLASSIFICATION OF ABSTRACT	20. LIMITATION OF ABSTRACT
UNCLASSIFIED	UNCLASSFIED	UNCLASSIFIED	

Final Technical Report on AFOSR-AASERT Project

Grant F49620-93-1-0555

on

Transport and Relaxation of Lubricant Fluids at High Pressure

by Principal Investigators:

J. Jonas and L. Ballard

Period Covered:

September 1, 1995 - January 31, 1997

CONTENTS

I. Summary of Research Accomplishments

A 300 MHz high resolution, high pressure (up to 9 kbar) NMR probe was built and tested. Specialized design features of the probe are discussed, and performance spectra exhibiting <1.0 Hz resolution are presented. A prototype 500 MHz high resolution, high pressure (up to 3 kbar) NMR probe was also built. It is important to point out that the performance features of these NMR probes are unique in the USA and the world.

A dynamic study of the polar fluids ethanol (ETOH) and 2,2,2-trifluoroethanol (TFETOH) confined to porous silica sol gel glasses is reported. The ^{13}CNMR spin-lattice relaxation times, T_1, were measured in glasses with pores ranging from 18.9 Å to 54.8 Å, over a temperature range of -13.6°C to 30.5°C. The data was analyzed in terms of the two-state, fast exchange model, and surface layer relaxation times, T_{1s}, were calculated. Using surface enhancement factors, T_{1b}/T_{1s}, where T_{1b} is the relaxation time of the bulk liquid, it was concluded that confinement has little effect on the internal rotation of terminal CF_3- or CH_3- groups, with a slight difference in the CF_3- behavior believed to be due to hydrogen bonding. A lower surface enhancement factor for the -CH_2- group of TFETOH compared to ETOH is believed to be related to the bulk transport properties resulting from the presence of fluorine.

In order to address the question of the effects of high acidity a NMR study of propionic and perfluoropropionic acids confined to porous silica glasses was also performed.

II. Research Accomplishments

II.1 High Resolution NMR Probe for Operating in the Pressure Range of 1bar to 9 kbar and at temperatures of -30° to 100°C

In our laboratory we built a new high pressure, high resolution NMR probe which has been used up to 8.25 kbar at a proton frequency of 300 MHz. The probe features a new feedthrough design that has been found to have a considerably extended life span compared to our earlier feedthrough designs. The proton circuit being used is double-tuned, containing a deuterium lock channel to maintain magnet stability over time. This makes the system quite suitable for high resolution studies requiring long acquisitions. In addition, the RF circuit being used in conjunction with this new feedthrough, which uses a tuning capacitor located inside the pressure vessel, has been found in bench tests to be capable of at least 500 MHz. This new probe will be used in studies of the dynamic structure of complex elastohydrodynamic (EHD) lubricants under extreme conditions such as high pressure. Some estimates describe the EHD regime as existing above 7 kbar, making higher pressure NMR probes a natural choice.

The new pressure vessel is shown schematically in Figure 1. The high strength beta alloy of titanium, 3Al-8V-6Cr-4Zr-4Mo (RMI Titanium, 180 kpsi YS), was used for the vessel body. The "soft" nature of this alloy, however, can lead to galling of titanium threads above 8 kbar. To prevent this, the top plug driver and the bottom plug were machined from full-hard Berylco 25 (NGK Metals Corp., 179 kpsi YS after heat treatment), which must be heat-treated 3 hours at 600°F before fine machining. The vessel's maximum outer diameter (2.75") is limited by the inner diameter of the room temperature shim coils, while the inner diameter (0.60") was chosen to accommodate an 8 mm sample tube and an RF coil. The vessel has a calculated ultimate burst pressure of 15.5 kbar at the sealing flanges, and has been pressure tested to 9.25 kbar, although actual

experimental NMR runs thus far have not exceeded 8.25 kbar. The top plug of the vessel is also of the beta titanium alloy, and contains up to three electrical feedthroughs.

Thermal control is provided by circulating 50/50 ethylene glycol/water through etched grooves in the exterior of the vessel. Temperatures inside the vessel are measured by a copper-constantan thermocouple encased in stainless steel (Omega Engineering, Inc.). The thermocouple enters the vessel through an additional feedthrough in the bottom plug, with a brazed stainless steel cone seated inside a copper cone providing the high pressure seal.

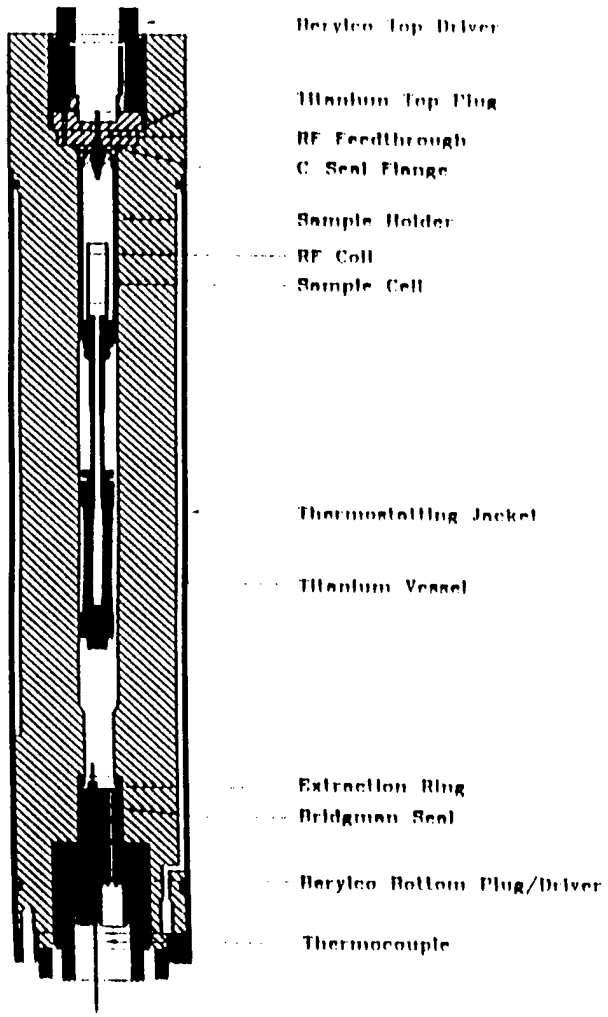

Figure 1. Schematic drawing of titanium high-pressure vessel used in the wide-bore-300 MHz superconducting magnet. For clarity, only one of the three feedthroughs is shown.

To demonstrate the high resolution possible with the new probe, we include data for our standard resolution sample containing 15% o-dichlorobenzene and 3% TMS in acetone-d_6. The proton spectrum for the aromatic region of this sample is shown in Figure 2. The resolution is based on the calculated linewidth at half-height of the TMS

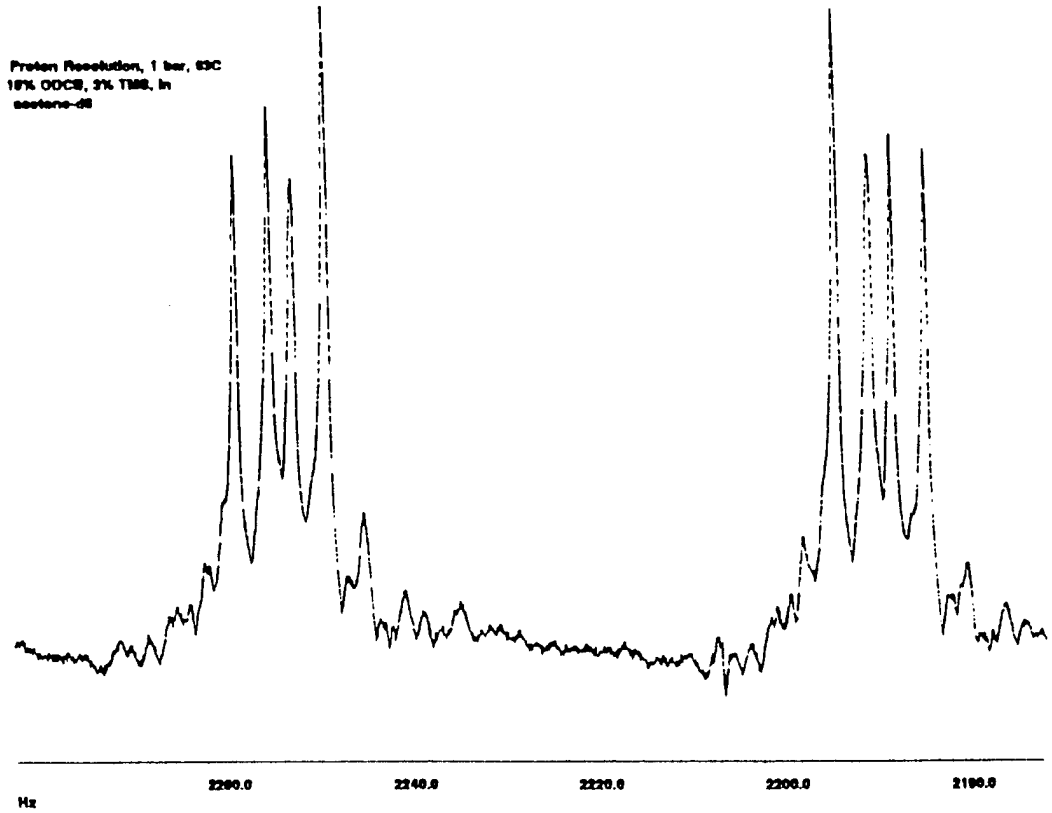

Fig. 2. The aromatic proton region of the 15% o-dichlorobenzene +3% TMS in acetone-d_6 sample used for the resolution test of the 300 MHz probe. The spectrum is taken at 1 bar and a temperature of 63°C.

peak. For the new probe, linewidths of < 1.0 Hz have been achieved, although linewidths of 1.5 Hz are typical for modest amounts of shimming. This resolution is independent of pressure up to 800 MPa, as is demonstrated by the 1 bar and 8 kbar TMS spectra shown in Figure 3. The typical high resolution ($5x10^{-9}$) is nearly identical to that of our commercial GE probe for a non-spinning sample ($4x10^{-9}$).

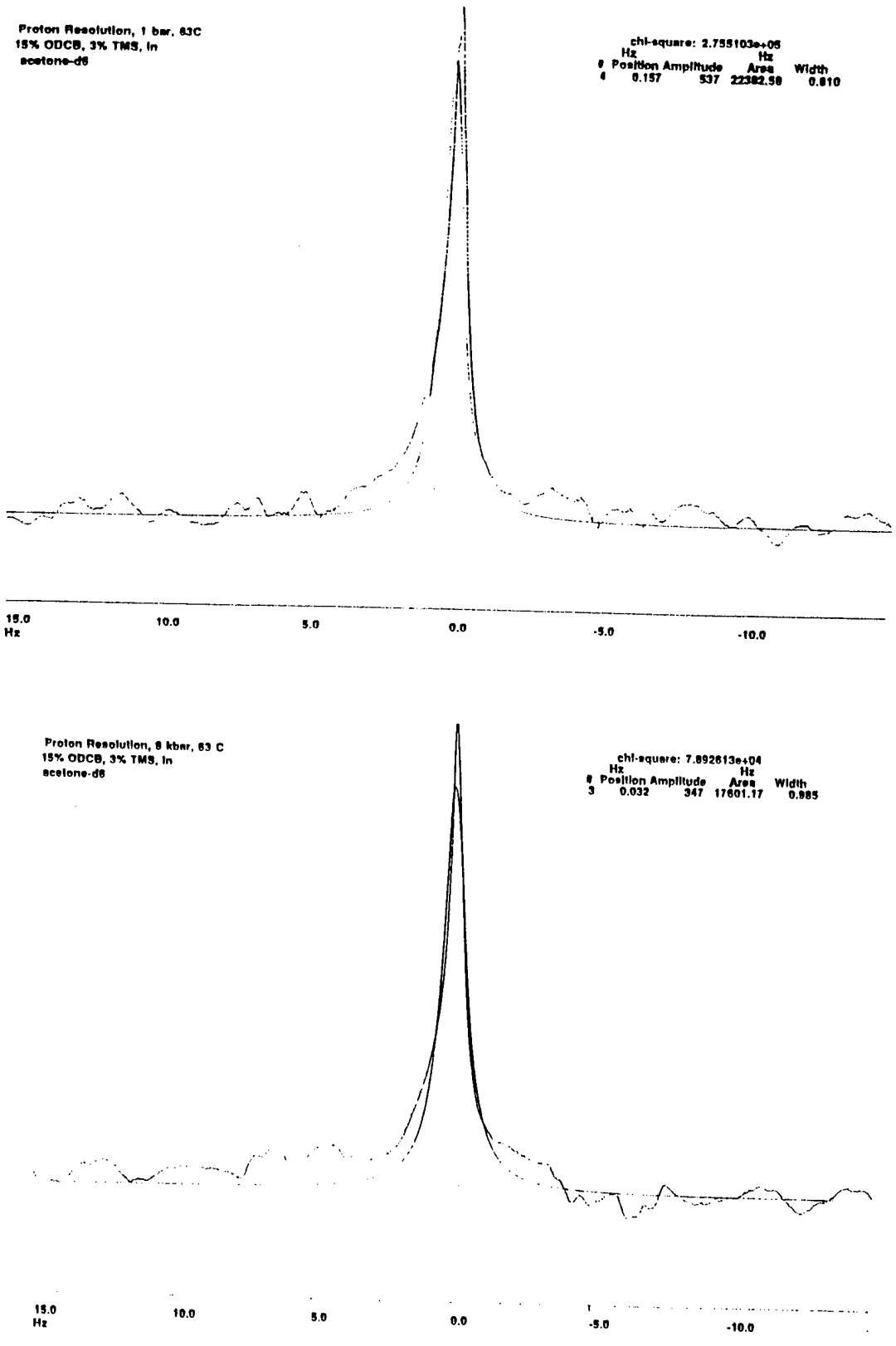

Fig. 3 The linewidth fitting of the TMS peak in the resolution sample (15% o-dichlorobenzene +3% TMS in acetone-d_6) at 63°C for (A) 1 bar; and (B) 8 kbar. The smooth line is the Lorentzain fitting result.

As a standard performance test, we routinely measure the sensitivity (S/N) of a 0.1% ethylbenzene, 0.2% TMS sample in chloroform-d sample for all of our probes. The measurement is performed at 1 bar using a 90° pulse and standard parameters, with S/N based on the relative height of the quartet region. Figure 4 shows a typical spectrum for the new probe. We must be cautious in comparing sensitivity with our commercial GE probe, as the commercial probe has an RF sample coil nearly twice that of our pressure probe. In addition, the high sensitivity of commercial probes can lead to dynamic range problems for strong peaks. With these concerns in mind, the typical S/N of 34:1 (8 mm tube, 90°=77μs) compares to our commercial GE probe value for the same sample of 265:1 (10 mm tube, 90°=22.5μs). Aside from the obvious difference in volume between

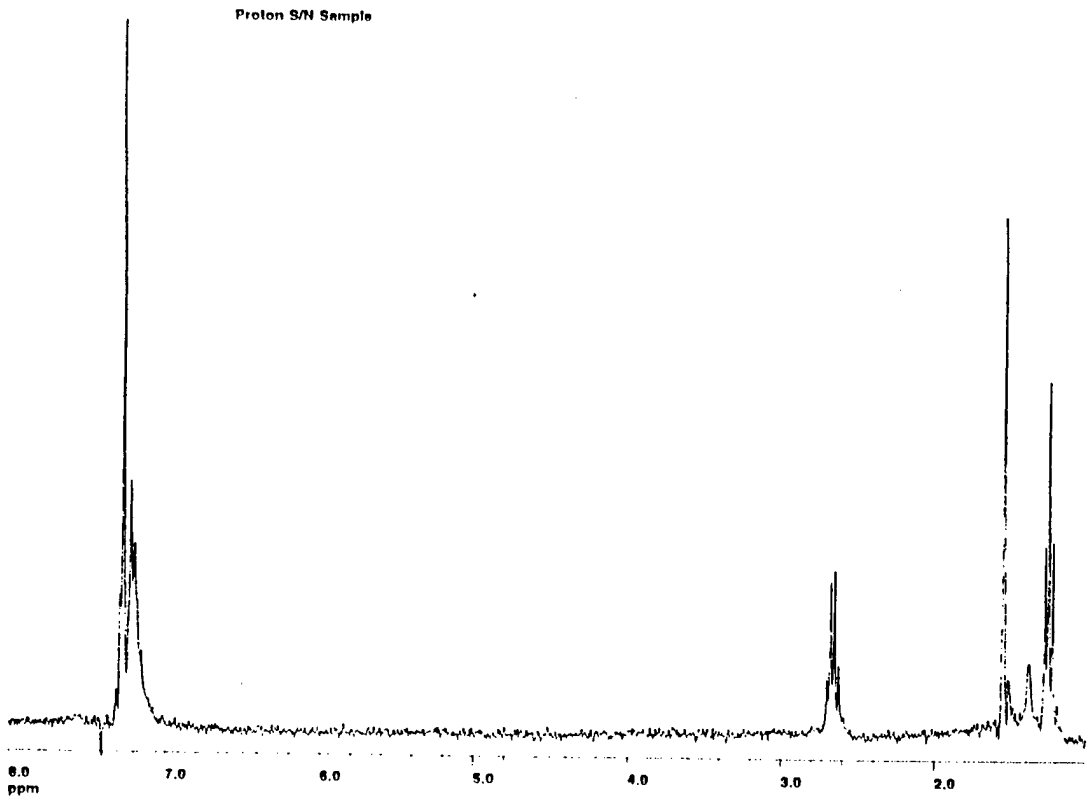

Fig. 4 The proton spectrum of 0.1% ethylbenzene +0.2% TMS in chloroform-d used for the S/N test of the 300 MHz probe.

the two sample tubes, most of the remaining difference in S/N is a natural consequence of losses due to the feedthrough. We should also point out that our optimization work aimed at improving the sensitivity continues.

II.2 500 MHz High-pressure, High Resolution NMR Probe

A new pressure vessel has been constructed of the beta 38-6-44 titanium alloy. The vessel was constructed with a longer length than any of our other pressure vessels, and can be interchanged between our 300 MHz magnet and the new 500 MHz magnet by simply exchanging probe stands. This utility is important, as it will allow for dynamic ^{13}C NMR T_1 measurements of liquids in 10 mm bellows assemblies on our 300 MHz system. The vessel design features a C-seal at its top connection, and a classic Bridgman seal on its bottom plug. The new vessel offers a compromise between strength and inner diameter, with a potential range of 7 kbar for a 10 mm tube. This is in contrast to our current 5 kbar (10 mm tube) and 9 kbar (8 mm tube) vessels.

A number of design modifications were introduced with the result that the 500 MHz probe has better than expected sensitivity and resolution. Specifically, at this point we shall mention the change in the use of the sample holder material.

A long-standing problem with our pressure probes has been control of baseline distortion and "glitches." While the problem can be minimized with proper software fitting of the baseline, it would still be much better (and make our data much more accurate) if the problem could be controlled at the source. Unfortunately, this problem is quite complex, and is believed to be the result of several phenomena, including low probe power, possible filter or digitizer mismatch, possible mixer "glitches," and probe sample

holder construction materials. Most of these sources are related to the system and are extremely difficult to isolate and identify.

One of the easy sources to examine, however, is distortions resulting from the

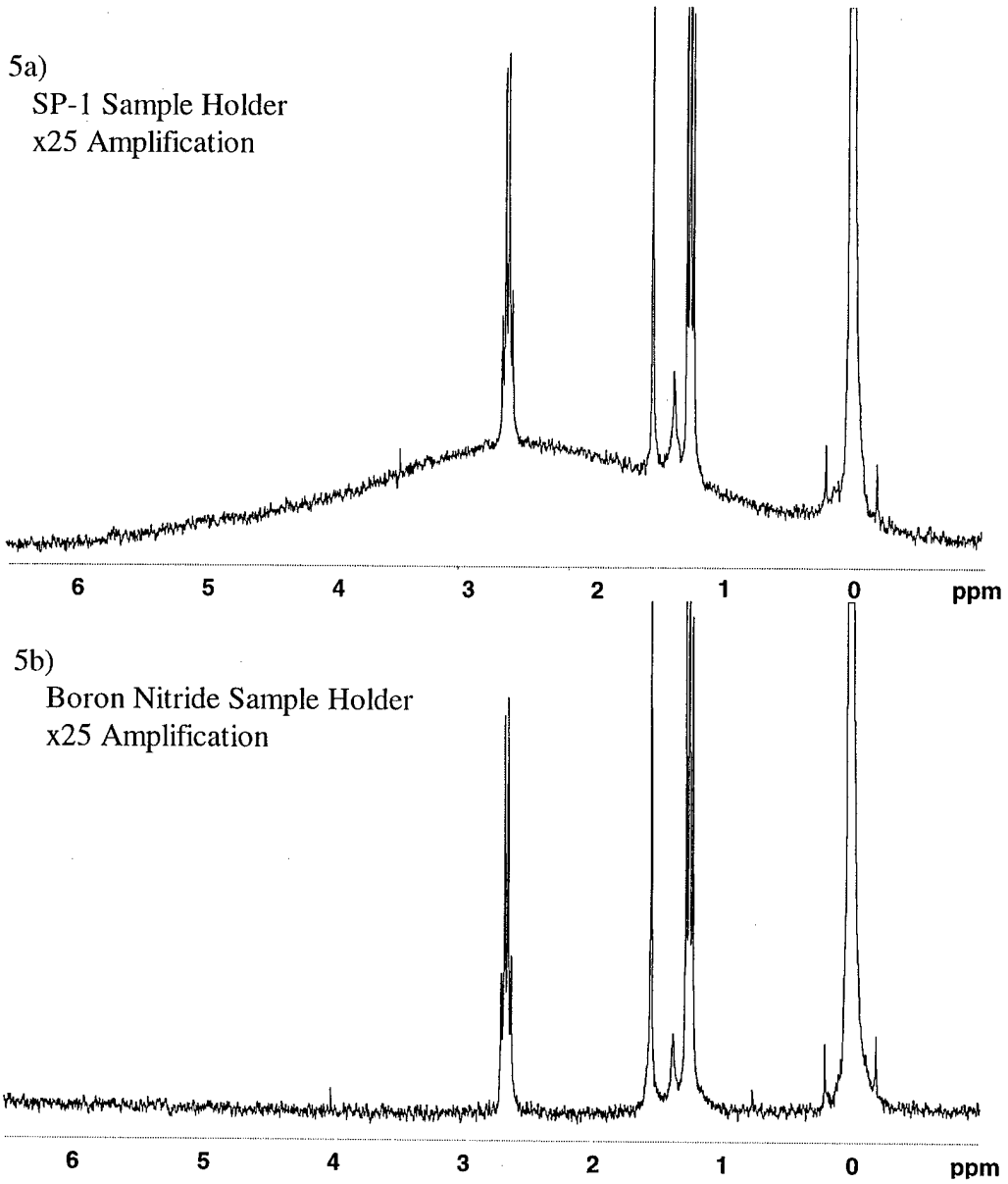

Figure 5. A comparison of the effects of the sample holder material for a) Vespel SP-1 and b) boron nitride. Both spectra are x25 amplified spectra of the standard S/N sample in the region of -0.5 to 6.5 ppm.

sample holder. Previously our sample holders have been constructed of the Vespel SP-1 (DuPont) polyimide which contains protons. Even though the proton signals for a plastic are broad, the fact remains that they are still there and introduce a "hump" in the alkane region of the spectrum which is shown in Figure 5a.

As an alternative to SP-1, new sample holders have been constructed of the ceramic Boron Nitride (BN). Figure 5b compares the "SP-1 hump region" for BN versus SP-1 sample holders. As one can clearly see, the hump has been completely eliminated in the ceramic.

But although the BN sample holders offer a significant advantage in the baseline, one is still faced with the problem of implementation. Unfortunately BN is quite brittle, and can easily crack if torqued too tightly to the titanium top plug. This limitation has forced a re-design of the top plug and the sample holder to allow for a much thicker BN wall.

II.3 Dynamic Behavior of Confined Liquid Acids

In addition to studies of bulk liquid fluorinated lubricants, the Air Force is also interested in studies of potential fluorinated lubricant additives which will obviously have to be included in lubricant formulations. One particular class of additives are the boundary layer lubricant additives which are believed to function by forming a molecular layer on engine parts, thereby preventing contact. In hydrocarbon lubricant packages, both alcohols and carboxylic acids are commonly used for boundary layer protection.

In our earlier study of ethanol (EtOH) versus 2,2,2-trifluoroethanol (TFE) in confinement, lower surface enhancement factors (SEF's or T_{1b}/T_{1s}) were measured for the fluorinated alcohol. For these two alcohol's, TFE is the stronger acid by virtue of its

electronegative fluorine constituents. An earlier vibrational study had concluded that these two alcohols participate in hydrogen bonding with silica surfaces as hydrogen bond acceptors, meaning that the electron-withdrawing nature of the electronegative fluorine constituents should cause TFE to form a weaker hydrogen bond to the silica surface. This explanation was also consistent with the ^{13}C NMR SEF results.

In contrast to weakly acidic alcohols such as EtOH and TFE which have pKa values higher than that of silica glass, a new study was sought comparing strong hydrocarbon versus fluorocarbon carboxylic acids in confinement. The system chosen was that of propionic acid (pKa ~ 4.7) versus pentafluoropropionic acid (pKa not known, but based on similar acids, probably ~ 0). While this study still features a fluorocarbon as the stronger acid, a couple of new "twists" are introduced:

a) The hydrocarbon is now the molecule which is closer to the silica glass in acidity; and,

b) These molecules have both a carbonyl group and a hydroxyl group, either of which may hydrogen bond to the surface hydroxyl groups of the silica.

Since the earlier study showed no statistically significant trends with temperature (and since the relaxation times of these molecules are sufficiently long to make additional studies extremely time consuming!), the intent from the start has been to economize time by performing this study at only one temperature.

Before discussing the results, it is appropriate to note *that an earlier vibrational study of propionic acid has concluded that hydrogen bonding with silica occurs through the oxygen atom of the carbonyl group*. This obviously would make the carboxylic acid serve as the hydrogen bond acceptor, just as with EtOH and TFE. Therefore, before

beginning, one might predict that trends similar to the EtOH/TFE study should be observed.

Propionic acid (Aldrich) and pentafluoropropionic acid (Aldrich) were received and used without further modification. The samples were handled under nitrogen, rigorously degassed with multiple freeze-pump-thaw cycles, and loaded under vacuum into porous silica sol gel glasses which had been dried for >2 hours under vacuum (<2.0 x 10^{-6} torr) at >300°C. The silica sol gel glasses ranged from 21 to 54 Å, as determined by BET analysis. After loading the pores, excess liquid was removed by application of vacuum and the sample tubes were flame-sealed. The procedure for loading samples has been described previously. Some additional samples were prepared using surface-modified glasses---those procedures and results will be presented at a future time.

^{13}C NMR experiments with either ^{1}H or ^{19}F CW decoupling were performed on a 4.7 Tesla magnet (proton frequency of 180 MHz) using a home-built spectrometer. Spin-lattice relaxation times (T_1) were measured at 25.3°C for each individual carbon atom using the inversion-recovery method with a 3-parameter exponential fit to account for imperfections in the 180° pulse. In all cases, at least three T_1 determinations were performed using a number of acquisitions appropriate for the sensitivity of the sample (4-256 scans). Temperature was controlled using a nitrogen stream regulated by a Lauda temperature bath and calibrated against the chemical shift change of a methanol standard. A limited number of additional T_1 measurements were performed on a commercial GN-300 MHz instrument at the SCS VOICE NMR lab to investigate chemical shift anisotropy contributions.

Table I contains the measured spin-lattice relaxation times for PPA and PFPPA in bulk liquid and confinement at 45.2 MHz, and the data is displayed in Figures 6 and 7. In addition, Table II contains bulk liquid relaxation times at various temperatures (Figures 8 and 9).

Table I. Spin-Lattice Relaxation Times (T_1) for Propionic Acid (PPA) and Pentafluoropropionic Acid (PFPPA) in Confinement at 25.3°C.

PPA			
Pore Radius (Å)	**C1 T_1 (s)**	**C2 T_1 (s)**	**C3 T_1 (s)**
bulk	27.9 (7)	5.40 (6)	5.79 (5)
54 (1)	7.4 (5)	1.89 (8)	4.5 (2)
34 (1)	9 (1)	1.43 (5)	4.2 (2)
27 (1)	7.0 (4)	1.13 (6)	3.6 (2)
21 (1)	6.0 (3)	0.86 (4)	3.3 (2)

PFPPA			
Pore Radius (Å)	**C1 T_1 (s)**	**C2 T_1 (s)**	**C3 T_1 (s)**
bulk	20.1 (8)	10.2 (1)	5.55 (8)
54 (1)	6.8 (7)	3.9 (2)	3.3 (2)
34 (1)	9.1 (8)	3.3 (2)	2.8 (2)
27 (1)	7 (1)	2.7 (2)	2.4 (1)
21 (1)	4.7 (6)	2.3 (2)	2.0 (1)

Number in parentheses () indicates the uncertainty in the last significant digit based on error propagation.

Table II. Spin-Lattice Relaxation Times (T_1) for Propionic Acid (PPA) and Pentafluoropropionic Acid (PFPPA) Bulk Liquid at Various Temperatures.

PPA Bulk Liquid			
Temperature (°C)	**C1 T_1 (s)**	**C2 T_1 (s)**	**C3 T_1 (s)**
1.4	23.3 (5)	3.35 (6)	4.05 (4)
15	26.9 (8)	4.51 (6)	5.08 (7)
25.3	27.9 (7)	5.40 (6)	5.79 (5)

PFPPA Bulk			
Temperature (°C)	**C1 T_1 (s)**	**C2 T_1 (s)**	**C3 T_1 (s)**
1.4	19.0 (5)	6.81 (9)	3.41 (8)
15	19.0 (7)	9.0 (2)	4.70 (9)
25.3	20.1 (8)	10.2 (1)	5.55 (8)

Number in parentheses () indicates the uncertainty in the last significant digit based on error propagation.

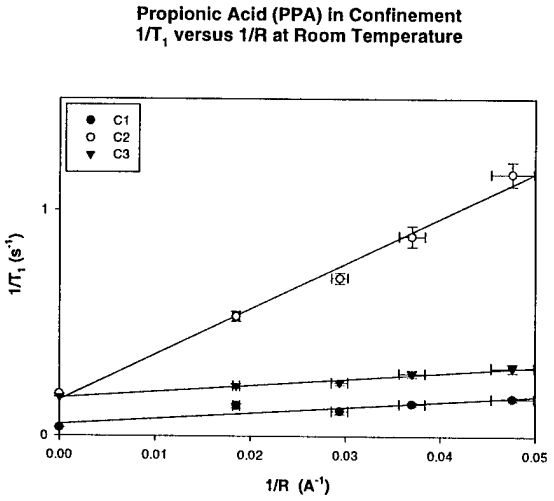

Figure 6. Confined geometry results for PPA at 25.°C

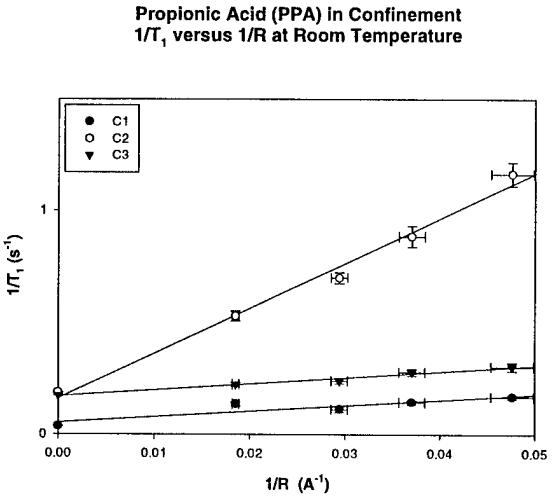

Figure 7. Confined geometry results for PPA at 25.°C.

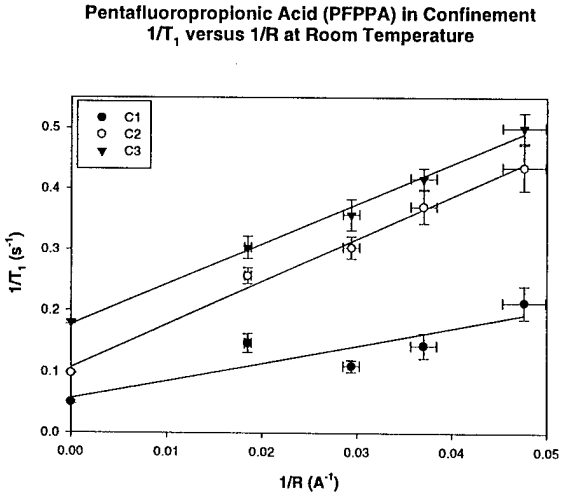

Figure 8. Confined geometry results for PFPPA at 25.3°C.

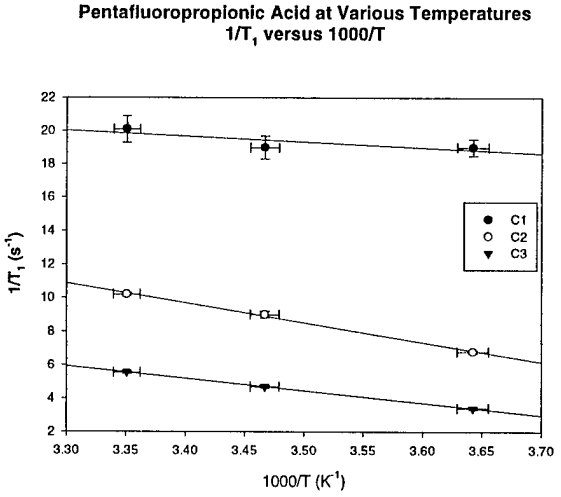

Figure 9. Bulk liquid results for PFPPA at various temperatures.

Molecular diameters are not currently available for these carboxylic acids, but are estimated to be ~4.75 and 5.0 Å for PPA and PFPPA, respectively, based on the diameters of EtOH and TFE. Using these estimates, surface-layer T_1 values for this polar system were computed using the two-state, fast-exchange model

$$\frac{1}{T_{1s}} = \frac{1}{T_{1b}} + \frac{2\varepsilon}{R}\left[\frac{1}{T_{1s}} - \frac{1}{T_{1b}}\right] \qquad (1)$$

where T_{1s} is the surface-layer spin-lattice relaxation time, T_{1b} is the bulk liquid relaxation time, ε is the molecular diameter, and R is the molecular radius. These values, as well as the SEF values, are compiled in Table III.

Table III. T_{1s} and SEF Values for PPA and PFPPA at Room Temperature.

PPA			
Parameter	**C1**	**C2**	**C3**
T_{1s} (s)	2.9 (3)	0.45 (1)	2.20 (5)
SEF	10. (1)	12.0 (3)	2.63 (6)

PFPPA			
Parameter	**C1**	**C2**	**C3**
T_{1s} (s)	2.8 (3)	1.22 (3)	1.21 (2)
SEF	7.2 (8)	8.4 (2)	4.6 (1)

Number in parentheses () indicates the uncertainty in the last significant digit based on error propagation.

Based on the SEF trends in Table III, some observations can be made. First, just as with the EtOH/TFE study, the terminal $-CH_3$ or $-CF_3$ has a much lower SEF. This trend is again expected since it appears that confinement has little effect on rapid internal rotation. In looking at both the C1 and C2 trends, one observes SEF's for the hydrocarbon which are higher than those of the fluorocarbon and again is consistent with the earlier EtOH/TFE study. It deserves noting, however, that the fluorocarbon in this case **does** appear to have slightly higher SEF's than TFE.

Thus, the conclusion of this study appears to again be that the presence of fluorine causes a weaker hydrogen bond interaction between the polar fluorocarbon and the silica surface, due to the fact that the acids are hydrogen bonding through their carbonyl oxygen atoms as hydrogen bond acceptors. This conclusion is consistent with the vibrational study of propionic acid which is in the literature, and with the trends observed for C1 and C2. The fact that the difference in SEF's between the fluorocarbon and the hydrocarbon

is less than in the alcohol study, however, may indicate that the disparity in hydrogen bonding strengths is smaller than in the earlier study.

II.4 Dynamic Structure of Ethanol and 2,2,2-Trifluorethanol Confined to Porous Silica Glasses

Recent emphasis in our laboratory has been on examining the role of fluorine in modifying the dynamic behavior of fluorocarbons versus hydrocarbons. Such emphasis should be of relevance to the lubrication process, especially as designers take advantage of the high thermal stability and relative chemical inertness of fluorocarbons, such as Krytox (Dupont) fluids. Attention must also be given to the new varieties of soluble additives that must be developed in conjunction with fluorinated lubricants. This includes studies dealing with simple, partially fluorinated alcohol's which can serve as boundary layer additives. Relevant examples are the systematic studies of Gellman, *et. al.*, such as a recent one examining the boundary lubricating ability of 2,2,2-trifluoroethanol. Gellman's work has been at least partially motivated by surprising earlier studies showing partially fluorinated surface films on silica tend to have higher friction coefficients in response to shear than non-fluorinated surface layers. This is in contrast to the known reduction in friction accompanying fluorinated PTFE's.

We carried out a ^{13}CNMR spin-lattice relaxation comparison of the polar molecules ethanol (ETOH) and 2,2,2-trifluoroethanol (TFETOH) in bulk liquid and confined to porous, sol gel silica glasses. This work follows a related comparison of non-polar methylcyclohexane and perfluoromethylcyclohexane. Our earlier work has shown theoretically how the confined geometry approach allows one to separate the relaxation rates of molecules in the "surface layer" from the bulk liquid. For liquids confined to

high-purity silica glasses, the observed relaxation rate is affected by interaction with the surface and by pure geometric (topological) confinement. This leads to the general expression for the observed spin-lattice relaxation, T_1 in a confined system

$$\frac{1}{T_1} = \frac{1}{T_{1b}} + \frac{2\varepsilon}{R}\left[\frac{1}{T_{1s}} - \frac{1}{T_{1b}}\right] - \frac{\varepsilon^2}{R^2}\left[\frac{1}{T_{1s}} - \frac{1}{T_{1b}}\right] + \frac{A(\omega)}{R^2} \qquad (2)$$

where T_{1b} is the bulk liquid spin-lattice relaxation time, T_{1s} is the surface layer spin-lattice relaxation time, ε is the thickness of the surface layer, R is the average pore radius, and $A(\omega)$ represents the topological confinement. When considering a polar system where surface interactions are strong, Equation (2) reduces to the familiar two-state, fast exchange model (Eq (1))

As Equation (1) shows, measuring relaxation rates over a range of pore radii allows one to determine the relaxation rate of the surface-layer liquid. One can proceed to calculate the surface enhancement factor, T_{1b}/T_{1s} or SEF, which emphasizes the relative differences in relaxation rates due to the surface. Thus, a relaxation study of a fluorocarbon versus a hydrocarbon should demonstrate dynamic differences at the glass/liquid interface introduced by fluorine. By selecting a nucleus such as ^{13}C, which is common to both molecules and whose relaxation mechanisms are well understood, one should have an added advantage in isolating the effect of fluorine.

Our main goal was to take advantage of ^{13}CNMR to compare and analyze the differences induced by fluorine in the surface enhancement factors for the individual carbon atoms of ETOH and TFETOH. This would allow greater understanding of how surface layer dynamics are influenced by polarity and fluorination. Although admittedly dealing with a system in the absence of shear, we also hoped to provide some insight into

the surface layer dynamics which might be applicable to the previously described boundary layer additive trends.

Decoupled spin-lattice relaxation times for each individual carbon atom in TFETOH and ETOH were determined over the temperature range of -15 to 30°C for bulk liquid samples and for samples confined to glasses with pores of 19 to 54 Å. Representative relaxation times at 21.3°C are listed in Table IV. NOE's determined at 75 MHz for the bulk liquid samples at the highest experimental temperatures exhibited 100% NOE (η=1.98) within experimental error, while T_1 values measured at 75MHz agreed within experimental error with values at 45.2 MHz.

TABLE IV. Observed T_1 Values (s) for ETOH and TFETOH at 21.3°C.

	ETOH		TFETOH	
Pore Size	C-1	C-2	C-1	C-2
bulk	9.85 (6)	7.1 (2)	2.73 (4)	6.45 (6)
54.8 Å	4.43 (9)	5.3 (1)	1.48 (6)	4.2 (3)
34.4 Å	3.2 (1)	4.6 (2)	1.14 (3)	3.5 (1)
27.7 Å	2.66 (7)	4.2 (1)	0.99 (2)	3.2 (4)
18.9 Å	1.96 (6)	3.3 (2)	0.71 (2)	2.3 (2)

Note: Values in parentheses represent the error in the last digit, representing the error from multiple runs or the accumulated T_1 fitting error.

For ^{13}CNMR, is has been established that spin lattice relaxation generally occurs by intra-molecular dipole-dipole relaxation, with occasional contributions from readily identifiable spin rotation and chemical shift anisotropy mechanisms. Based on the increase in T_1 with temperature observed, one can rule out spin rotation over the temperature range studied. In addition, the NOE values and the high field relaxation times tend to rule out chemical shift

anisotropy contributions. This leaves intra-molecular dipole-dipole relaxation as the dominant relaxation mechanism.

With a relaxation mechanism determined, one can proceed with data analysis. For this analysis, a surface layer of one molecular diameter was assumed. Molecular diameters were calculated by the fluidity analysis method of Hildebrand and Lamoureaux using viscosity and density data from the literature. By using these values and plotting the relaxation rate (T_1^{-1}) versus the inverse pore radius (R^{-1}), Equation (1) can be used to calculate surface layer relaxation times, T_{1S}. These plots are shown in Figures 10 and 11, and the calculated T_{1S} values are listed in Table V. The surface enhancement factors (SEF's or T_{1b}/T_{1S}) are also listed in Table V. Except for C-1 of TFETOH, the SEF's generally decrease with increasing temperature. One notes from Table V that the ETOH C-1 SEF is nearly twice that of TFETOH, while the TFETOH C-2 SEF is slightly greater than that of ETOH. For both liquids, the C-1 SEF is greater than C-2.

While the apparent trends in SEF's are interesting, we feel their explanation may be related to previous studies in our laboratory. First, we believe that the lower SEF values for C-2 versus C-1 indicate that relaxation occurring through internal rotation about the CF_3- or CH_3- groups is not affected greatly by confinement or surface interaction. This is in contrast to overall molecular motion, which is influenced. Such a description supports an explanation we proposed for acetonitrile in which we reported diffusion about acetonitrile's central symmetry axis was not greatly affected by confinement. We also note the connection with our pressure studies of acetonitrile, both in bulk and in confinement, in which similar results for the CH_3- group were obtained

If the C-2 SEF's were completely unaffected by fluorine, no difference in SEF values for CF_3- versus CH_3- would be expected. The fact that the CF_3- SEF is higher indicates this is not completely true. In explaining our previous results, we had suggested that local dipole-dipole interactions were the reason for higher surface enhancement factors for nonpolar perfluoromethylcyclohexane versus methylcyclohexane. Such an

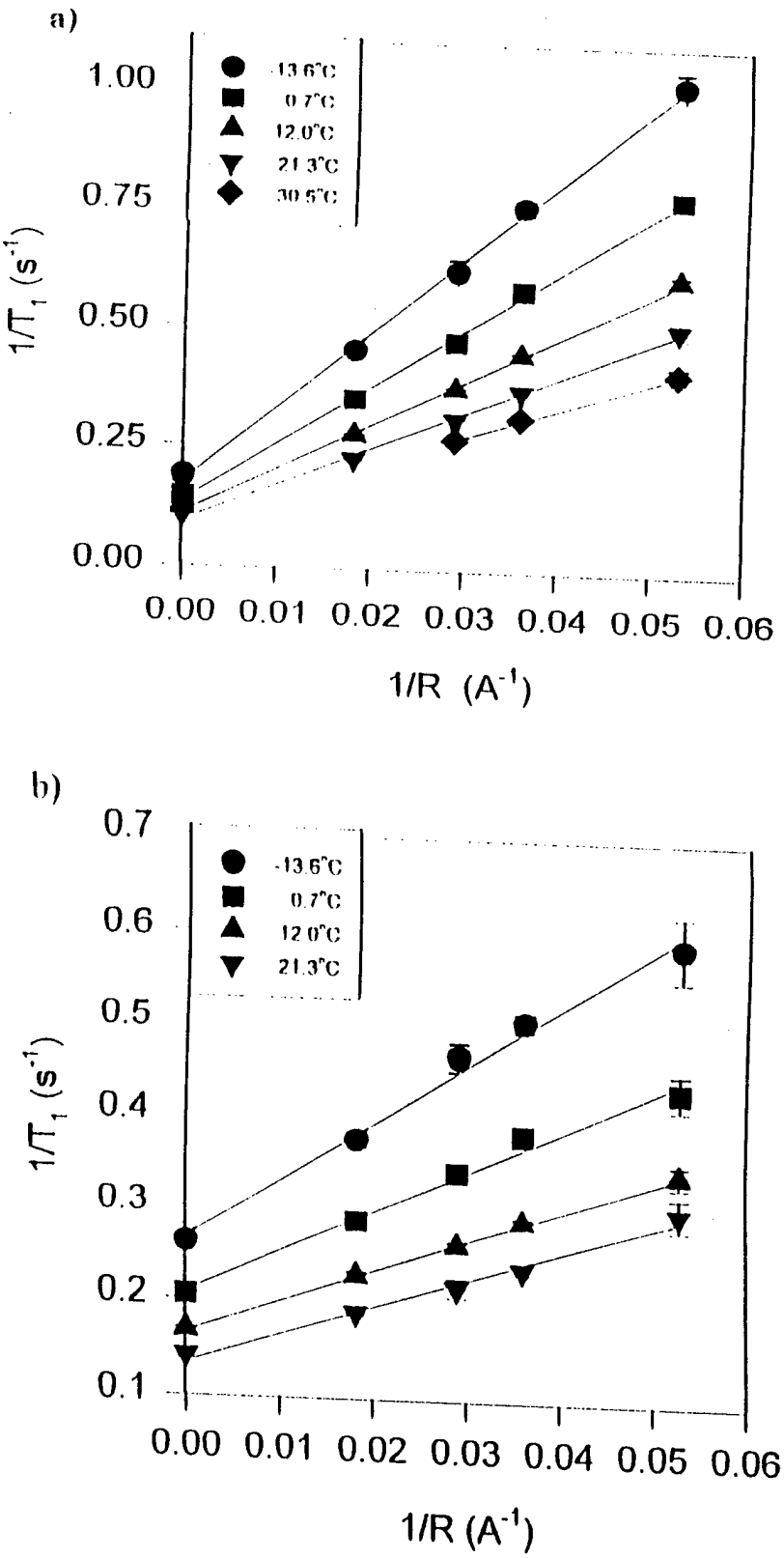

Figure 10. Ethanol plots of $1/T_1$ versus 1/R for C-1 (a) and C-2 (b). Error bars not shown fall into symbols.

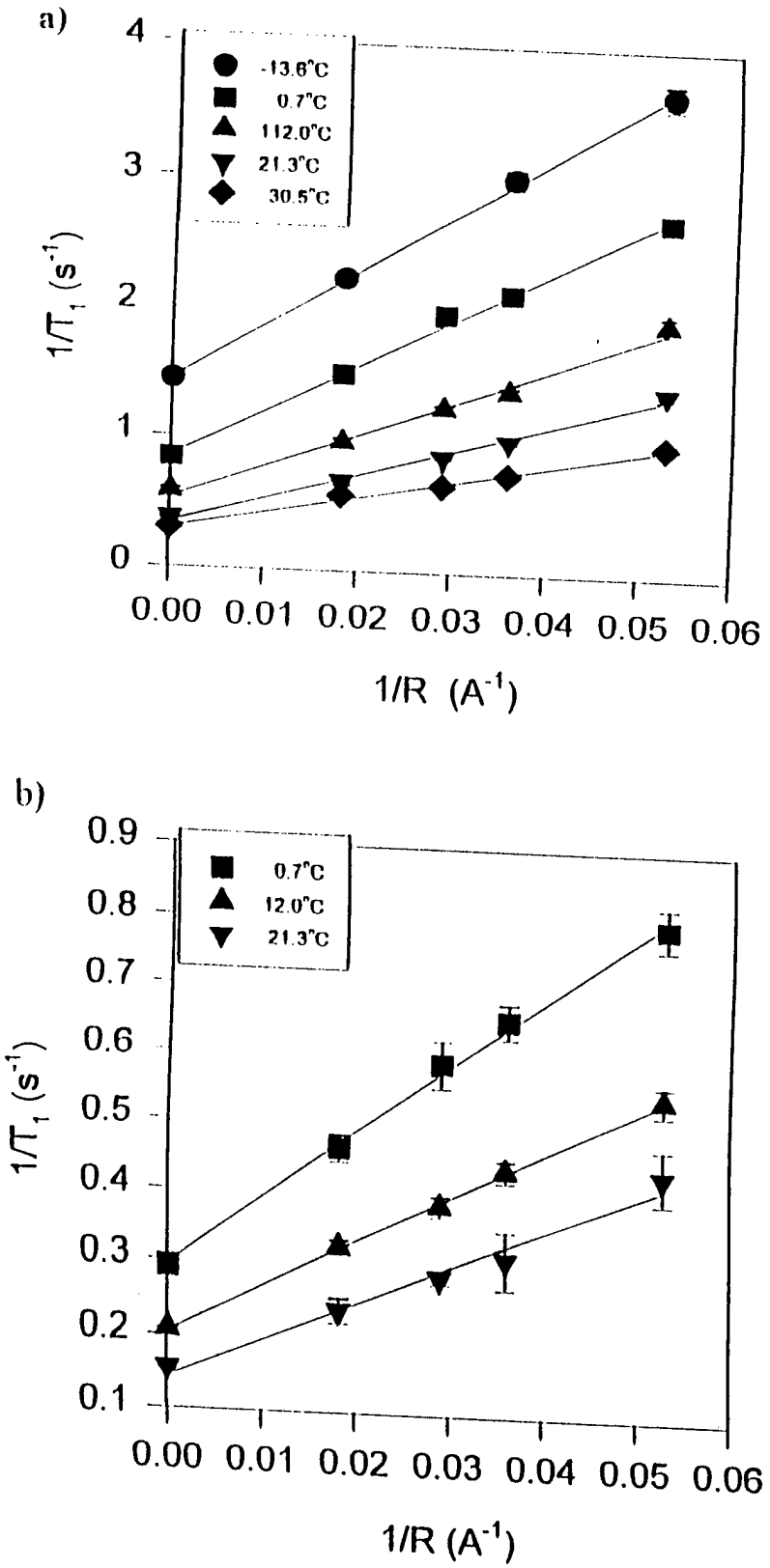

Figure 11. 2,2,2-Trifluoroethanol plots of $1/T_1$ versus 1/R for C-1 (a) and C-2 (b). Error bars not shown fall into symbols.

explanation would also explain our current result, although we deem it is unlikely given the strength of -OH interactions with the surface. Instead, we believe the explanation for the observed behavior of these polar molecules is TFETOH's known barrier to rotation. This barrier suggests for our study that the surface layer $-CF_3$ group is hydrogen-bonding with -OH groups on the silica surface, or with the bulk liquid -OH groups, thereby hindering rotation and giving TFETOH's C-2 a higher SEF than ETOH.

The C-2 trends are of interest because they demonstrate differences due to the effect of directly attached fluorine. The C-1 atoms, though, should be equally interesting since they should demonstrate differences due to polarity. Unlike the C-2 atoms which can relax through the internal rotation, the C-1 atoms are "anchored," having their movement restricted by the strength of the -OH group's hydrogen bond with the surface.

TABLE V. Calculated T_{1S} (s) and Surface Enhancement Factors for ETOH and TFETOH.

	ETOH T_{1S} (SEF)		TFETOH T_{1S} (SEF)	
	C-1	C-2	C-1	C-2
-13.6°C	0.52 (10.3)	1.02 (3.8)	0.17 (4.2)	n.a.
0.7°C	0.68 (10.4)	1.40 (3.5)	0.21 (5.6)	0.75 (4.6)
12.0°C	0.87 (9.9)	1.85 (3.2)	0.32 (5.6)	1.14 (4.3)
21.3°C	1.06 (9.3)	2.17 (3.3)	0.42 (6.5)	1.48 (4.4)
30.5°C	n.a.	n.a.	0.59 (5.9)	n.a.

Note: Fitting error for T_{1S} values in all cases was <5%.

II.5 ^{13}C NMR Study of Temperature Effects on Several Polyalkylperfluoroether Lubricant Fluids

One of the longer running objects we have been involved with is the dynamic study of polyperfluorinated alkyl ethers (PPFAE's) by ^{13}C NMR. In previous reports, the motives and background have been outlined for this project---these will not be repeated here. For the past several months, work has been progressing on an ambient pressure, variable temperature comparison of five PPFAE's---Krytox 143 AX, Krytox 143 AY, Krytox 143 AZ, Demnum, and Fomblin Z. These experiments have primarily been performed on the 180 MHz instrument, but some studies have also been performed for Krytox 143 AY (branched-chain PPFAE) and Demnum (linear PPFAE) on the 300 MHz instrument at the VOICE NMR Lab. T_1 values were measured for the various PPFAE's (see Figure 12 for the polymer "repeating unit") with the decoupler set at two different positions. This procedure is necessitated by the large chemical shift range of ^{19}F. Yet while this clearly causes problems in the amount of time required for the experiment, one benefit is that one can also obtain fairly complete sets of data both with and without decoupling. This variable leads to some small differences in the theoretical models for relaxation, which may possibly be exploited in further attempts at verifying certain correlation models. In addition to this possibility, experiments performed on representative samples for branched versus linear PPFAE's at 300 MHz (^1H) can also be used to test correlation models.

At this time, nearly all of the T_1 data has been processed. Figures 13-17 contain some representative examples of these values for Krytox 143 AX, Krytox 143 AY,

Krytox 143 AZ, Demnum at 180 MHz (with and without decoupling), and Demnum at 300 MHz (without decoupling only). A number of additional similar curves exist for these oils with different decoupler settings, and for the Fomblin oil, which are not included in this report. While in most cases the data looks reasonable, unfortunately the process of ***formally*** fitting the data to various correlation models is only just beginning. These fitting attempts have been hampered somewhat by the probable need to weight the data according to the number of points collected (i.e., at lower temperatures fewer points were collected and thus the data should be weighted less heavily). This is a problem which can be overcome, but it will require some additional time for adjustments to the fitting routines. Therefore, it is not appropriate at this time to present only partial analysis of the fittings before all of the data is analyzed. It should be noted, however, that Cole-Davidson fitting of the Krytox series (test of molecular weight) shows an increase in correlation times consistent with the viscosity increases, but very little change in β values (which is what was expected!). Comparison of the branched to linear PPFAE's is too preliminary to comment on. Again, a formal write-up of these results will be made in the near future.

Krytox 143 Series Repeating Unit

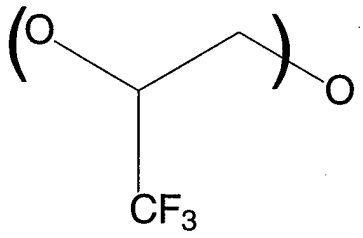

(completely fluorinated)

Demnum Series Repeating Unit

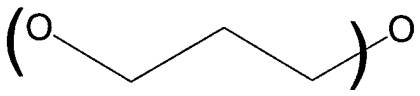

(completely fluorinated)

Fomblin Series Repeating Units

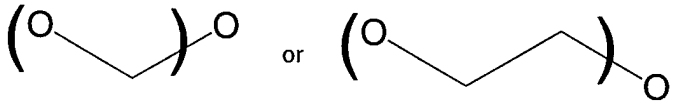

(completely fluorinated)

Figure 12. Repeating Units for the various PPFAE's

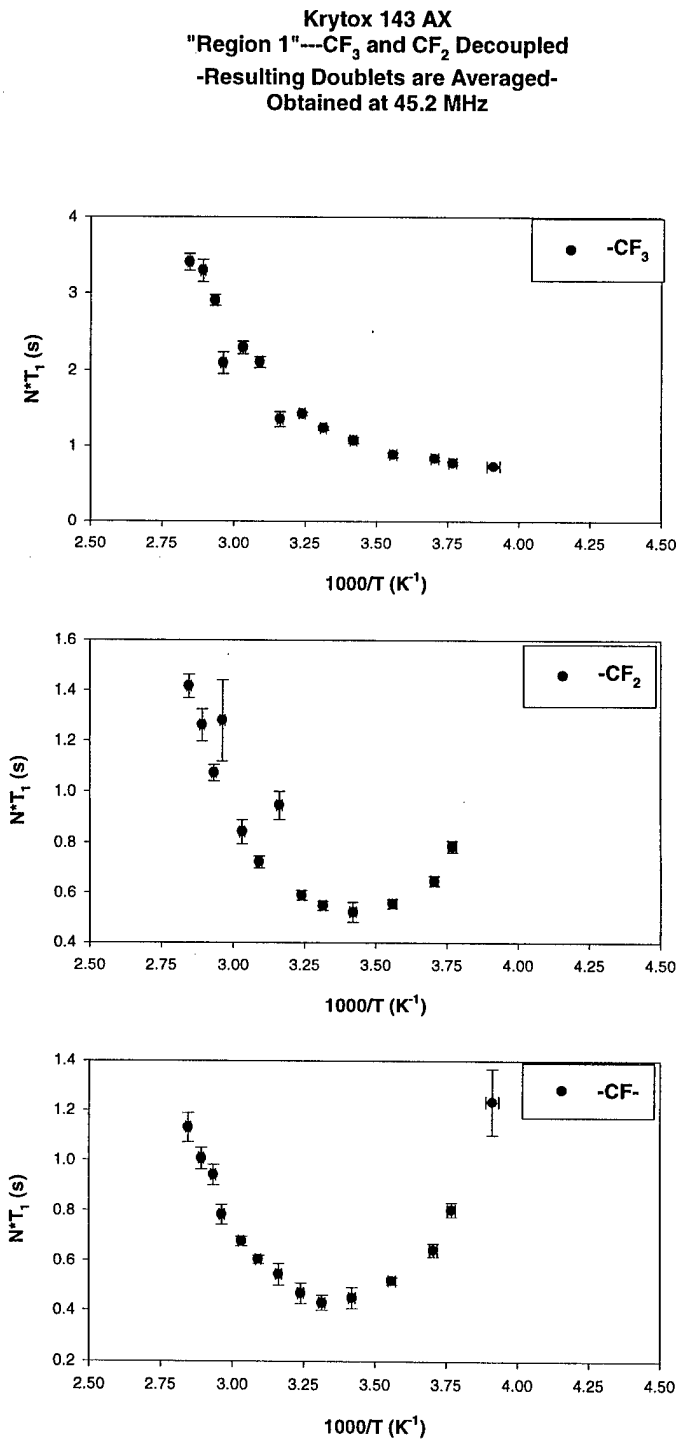

Figure 13. Krytox 143 AX ^{13}C NMR T_1 values with -CF_3 and -CF_2 Decoupled.

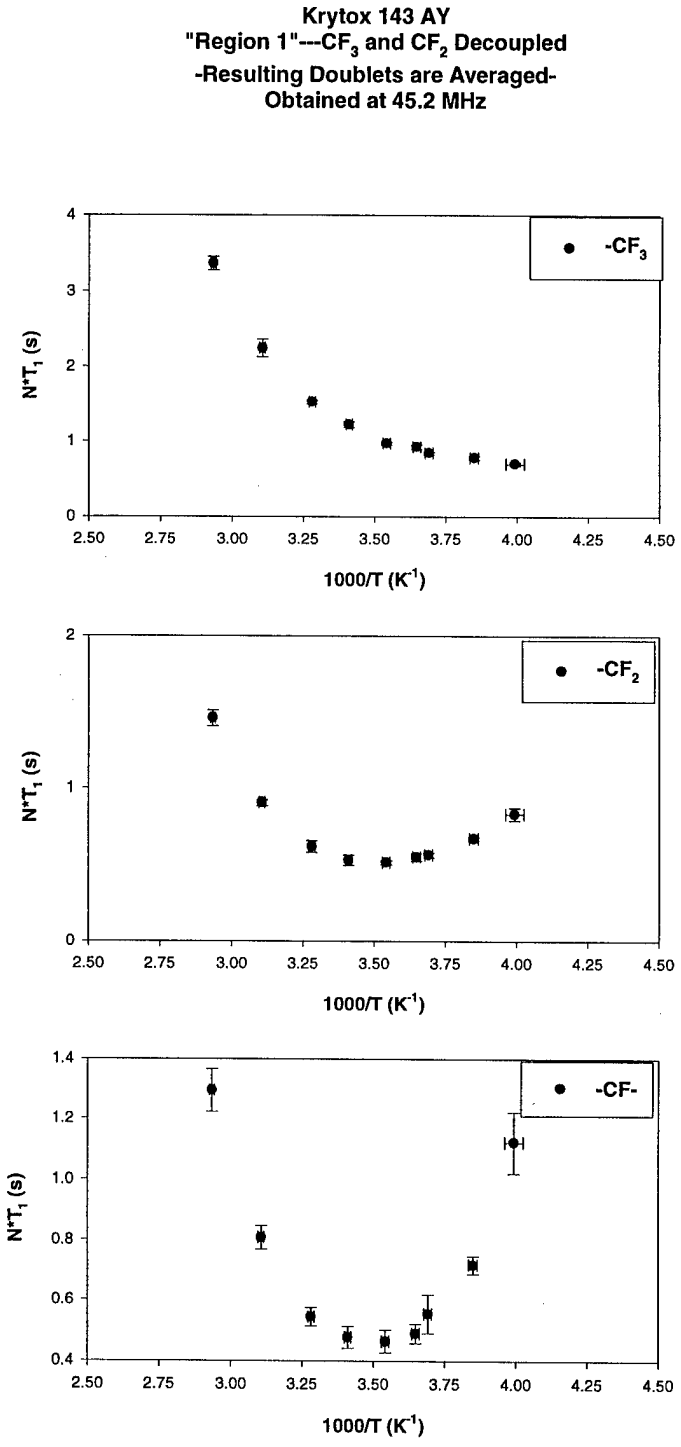

Figure 14. Krytox 143 AY ^{13}C NMR T_1 values with $-CF_3$ and $-CF_2$ Decoupled.

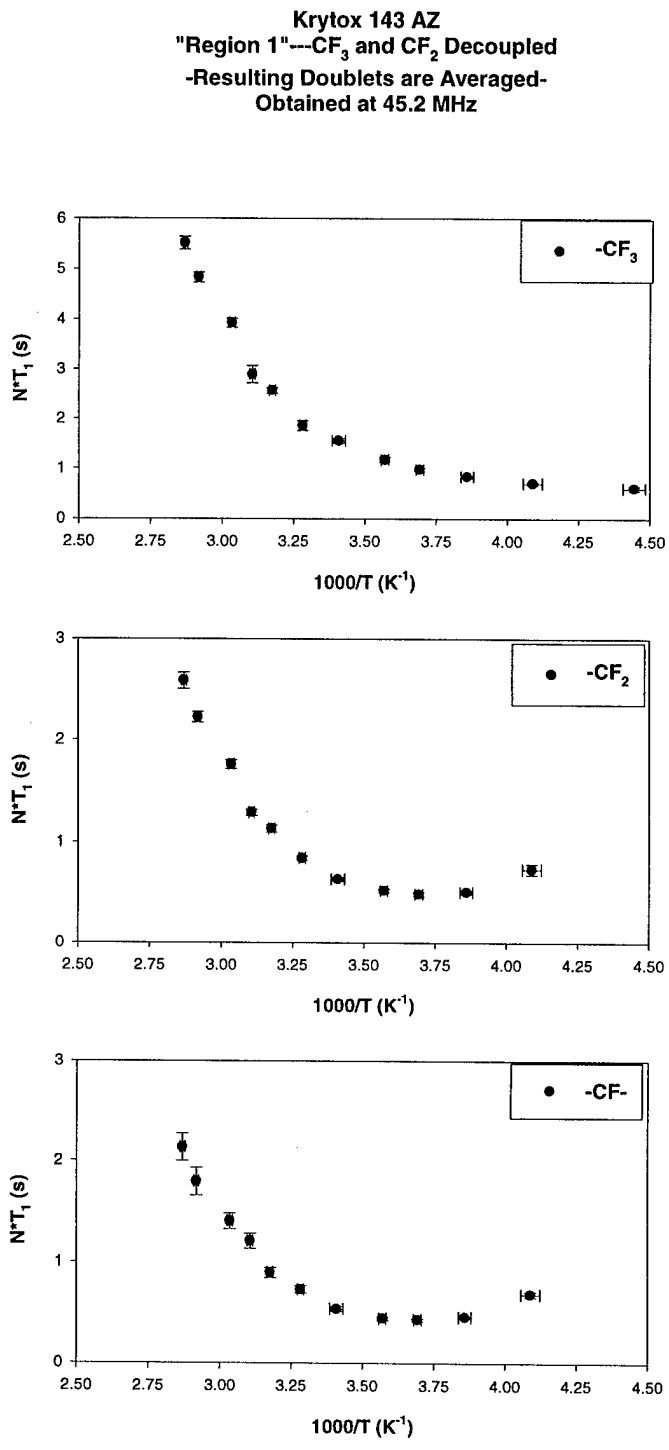

Figure 15. Krytox 143 AZ ^{13}C NMR T_1 values with $-CF_3$ and $-CF_2$ Decoupled.

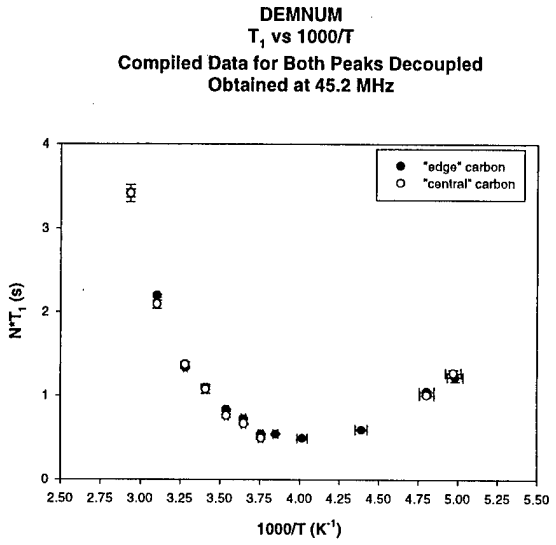

Figure 16. Demnum ^{13}C NMR T_1 values with temperature for carbon atoms decoupled, obtained at 45.2 MHz..

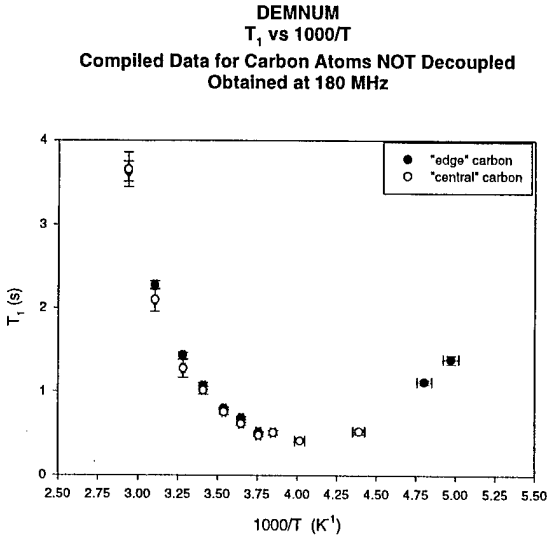

Figure 17. Demnum ^{13}C NMR T_1 values with temperature for carbon atoms NOT DECOUPLED, obtained at 45.2 MHz.

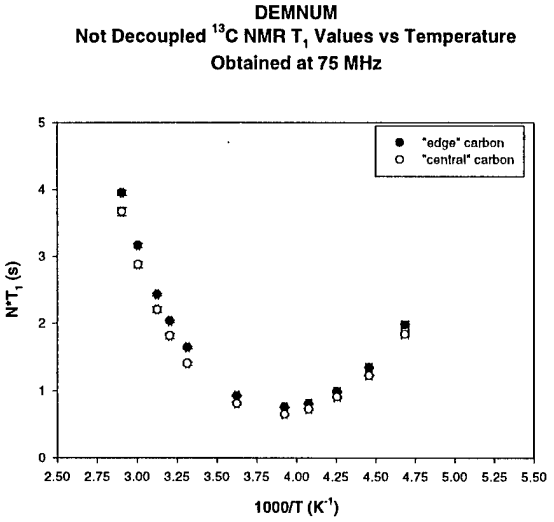

Figure 18. Demnum ^{13}C NMR T_1 values with temperature for carbon atoms NOT DECOUPLED, obtained at 75 MHz.

III. Personnel Supported:

Lance Ballard (Graduate Research Assistant)

IV. Publications:

"Dynamic Structure of Methylcyclohexane and Perfluoromethylcyclohexane Liquids in Confinement and in Bulk," S. Xu, L. Ballard, Y. J. Kim, and J. Jonas, J. Phys. Chem. 99, 5787-5792 (1995).

"NMR Study of Molecular Dynamics of Ethanol and 2,2,2-Trifluoroethanol Liquids Confined to Nanopores of Porous Silica Glasses," L. Ballard and J. Jonas, Langmuir 12, 2798-2801 (1996).

"High Pressure NMR," L. Ballard and J. Jonas, Annual Reports on NMR Spectroscopy, Vol. 33, Chap. 3, 115-150 (1997).

"High Resolution NMR Probe for Experiments at High Pressures," L. Ballard, C. Reiner, and J. Jonas, J. Magn. Res., 123, 81-86 (1996).

"Dynamic Structure of Propionic Acid Pentafluoropropionic Acid in Confinement and in Bulk Liquid," L. Ballard and J. Jonas, Manuscript in Preparation.

"^{13}C NMR Relaxation Study of the Dynamics of Polyperfluorinated Alkyl Ethers Lubricant Fluids," L. Ballard and J. Jonas, Manuscript in Preparation.

V. Interactions/Transitions

See Progress Report for F49620-93-1-0241

VI. New Discoveries, Inventions or Patent Disclosures

None